© 2022. Published by The Company of Biologists Ltd | Development (2022) 149, dev200917. doi:10.1242/dev.200917

RESEARCH ARTICLE

Heterologous expression of a lycophyte protein enhances angiosperm seedling vigor

Samuel W. H. Koh[1], Harold Nicholay Diaz-Ardila[1], Carlisle S. Bascom[2], Eduardo Berenguer[3], Gwyneth Ingram[3], Mark Estelle[2] and Christian S. Hardtke[1,*]

ABSTRACT

Seedling vigor is a key agronomic trait that determines juvenile plant performance. Angiosperm seeds develop inside fruits and are connected to the mother plant through vascular tissues. Their formation requires plant-specific genes, such as *BREVIS RADIX* (*BRX*) in *Arabidopsis thaliana* roots. BRX family proteins are found throughout the euphyllophytes but also occur in non-vascular bryophytes and non-seed lycophytes. They consist of four conserved domains, including the tandem BRX domains. We found that bryophyte or lycophyte BRX homologs can only partially substitute for *Arabidopsis* BRX (AtBRX) because they miss key features in the linker between the BRX domains. Intriguingly, however, expression of a BRX homolog from the lycophyte *Selaginella moellendorffii* (SmBRX) in an *A. thaliana* wild-type background confers robustly enhanced root growth vigor that persists throughout the life cycle. This effect can be traced to a substantial increase in seed and embryo size, is associated with enhanced vascular tissue proliferation, and can be reproduced with a modified, SmBRX-like variant of AtBRX. Our results thus suggest that BRX variants can boost seedling vigor and shed light on the activity of ancient, non-angiosperm BRX family proteins.

KEY WORDS: *Arabidopsis*, *Selaginella*, *Marchantia*, *Physcomitrium*, Vigor, Seed, Embryo, Root, Phloem, BRX

INTRODUCTION

Plant evolution is marked by major transitions that have led to the angiosperms, the flowering seed plants that dominate the extant terrestrial biosphere (Amborella Genome Project, 2013; Rensing, 2020; Spencer et al., 2021). Key developments include the evolution of vascular tissues, which separate lycophytes from the bryophytes; enclosure of the embryo in a seed, which separates spermatophytes from ferns; and protection of the seeds inside fruits, which separates angiosperms from gymnosperms. The development of such evolutionary novelties often entails plant-specific gene families (Armisén et al., 2008; Guo, 2013; Jiao et al., 2020; Pfannebecker et al., 2017; Rensing, 2020). Among them, the BREVIS RADIX (BRX) gene family comprises five members in the angiosperm model plant *Arabidopsis thaliana*, *AtBRX* and its homologs *AtBRX-LIKE* (*AtBRXL*) *1-4* (Beuchat et al., 2010a; Briggs et al., 2006). The encoded BRX family proteins consist of four distinct, highly conserved domains, which are not found outside the green lineage (Briggs et al., 2006; Koh et al., 2021). They include the signature tandem BRX domains, which are connected by a linker of variable sequence and size (Koh et al., 2021). Originally, *AtBRX* was identified based on a rare natural loss-of-function variant that might confer an adaptative advantage in certain conditions (Gujas et al., 2012; Mouchel et al., 2004; Shindo et al., 2008). Moreover, a rare *AtBRX* gain-of-function allele that carries a deletion in the linker between the BRX domains is associated with slightly increased root growth vigor (Beuchat et al., 2010a). *BRX* family gene variants have also been implicated in *Brassica* domestication (Zhang et al., 2021). These independent findings suggest that allelic variations in BRX family genes are relevant for the evolution of trait diversity.

All BRX family proteins monitored to date are primarily associated with the plasma membrane and display polar cellular localization (Bringmann and Bergmann, 2017; Koh et al., 2021; Marhava et al., 2020; Marhava et al., 2018; Scacchi et al., 2009). The biological functions of BRX family genes are diverse and point to sub-functionalization of individual family members (Koh et al., 2021; Li et al., 2019; Marhava et al., 2020; Zhang et al., 2021). For instance, the best-characterized members, *AtBRX* and *AtBRXL2*, are interchangeable in stomata development but not in root protophloem development (Koh et al., 2021; Marhava et al., 2020), and this unequal redundancy has recently been associated with differences in protein behavior (Koh et al., 2021; Marhava et al., 2020). In the root, AtBRX guides the progression of protophloem sieve element differentiation by modulating the local trans-cellular flux of the phytohormone auxin (Marhava et al., 2018; Moret et al., 2020). In *brx* loss-of-function mutants, protophloem differentiation is thus impaired and, consequently, root growth vigor is strongly reduced (Anne and Hardtke, 2018; Moret et al., 2020; Mouchel et al., 2004; Rodrigues et al., 2009). The AtBRX protein is polarly localized at the rootward end of developing protophloem sieve elements, where it interacts with an AGC-type kinase regulator of the auxin transport machinery in an intricate, feedback-regulated 'molecular rheostat' (Aliaga Fandino and Hardtke, 2022; Bassukas et al., 2021; Marhava et al., 2018). A key feature of this molecular rheostat is the auxin-responsive plasma-membrane dissociation of AtBRX (Marhava et al., 2018; Scacchi et al., 2009), which is a quantitative determinant of BRX family protein activity in the developing protophloem (Koh et al., 2021; Marhava et al., 2020). This feature has been mapped to AGC kinase target phosphosites, including a key site in the linker sequence between BRX domains, and these phosphosites are present in AtBRX but absent in AtBRXL2 (Koh et al., 2021). Engineering these sites into AtBRXL2 renders the modified protein auxin-responsive and augments its biological activity in the protophloem (Koh et al., 2021). Conversely, in a BRX family

[1]Department of Plant Molecular Biology, University of Lausanne, CH-1015 Lausanne, Switzerland. [2]Section of Cell and Developmental Biology, University of California San Diego, La Jolla, CA 92093, USA. [3]Laboratoire Reproduction et Développement des Plantes, ENS de Lyon, 69364 Lyon, France.

*Author for correspondence (christian.hardtke@unil.ch)

C.S.H., 0000-0003-3203-1058

Handling Editor: Ykä Helariutta
Received 6 May 2022; Accepted 26 September 2022

Development (2022) 149, dev200917. doi:10.1242/dev.200917

protein from the lycophyte *Selaginella moellendorffii* (SmBRX), the phosphosites are missing and the linker is much shorter than in *A. thaliana* BRX family proteins (Koh et al., 2021). Thus, SmBRX plasma-membrane association is not auxin-responsive and can only partially rescue the protophloem differentiation defects of *brx* loss-of-function mutants (Koh et al., 2021). In summary, the available data suggest that sub-functionalization of BRX family proteins is at least in part determined by the sequence of the linker between the tandem BRX domains.

Despite their inability to fully complement the *brx* mutant, both AtBRXL2 and SmBRX can confer significant rescue of average root growth vigor when expressed under the control of the *AtBRX* promoter (Beuchat et al., 2010a; Briggs et al., 2006; Koh et al., 2021). This might reflect the significant yet partial rescue of protophloem defects, which manifests in a strongly reduced proportion of seedlings that display visibly impaired differentiation in both sieve element strands, suggesting that at least one strand is often functional (Breda et al., 2017; Koh et al., 2021). Nevertheless, compared with other BRX family proteins that lack the key AGC kinase target phosphosite in the linker and were monitored previously (Beuchat et al., 2010a; Briggs et al., 2006; Marhava et al., 2020), the rescue of *brx* root growth vigor obtained with SmBRX was remarkable and statistically indistinguishable from that of the Columbia-0 (Col-0) wild-type control (Koh et al., 2021). Here, we explored this phenomenon in detail and found that SmBRX expression in *A. thaliana* wild type substantially enhances seedling vigor.

RESULTS

The linker between the BRX-domains determines BRX protein family sub-functionalization

Alignment of 300 full-length bona fide BRX family proteins retrieved from across the green lineage (One Thousand Plant Transcriptomes Initiative, 2019) shows that the key AGC target phosphosite (corresponding to S228 in AtBRX) is embedded in a 20-amino-acid motif within the linker (SAXXSPVTPPLX-KERLPRNF), which is conserved in the majority of BRX family proteins (supplementary Dataset 1; Fig. S1). Although the phosphosite serine shows the highest level of conservation (89%) within this motif, the AGC kinase consensus motif [R(D/E)S] is only present in a subset of ∼10% of BRX family proteins, which are all exclusively from angiosperms. Moreover, in AtBRX and its functionally interchangeable homolog AtBRXL1 (Briggs et al., 2006; Koh et al., 2021), the R(D/E)S site is present but the motif is only partly conserved. Finally, the motif is notably absent from all lycophyte and bryophyte BRX family proteins examined.

To further determine the functional relevance of this region, we chose to investigate a few representative BRX family proteins from different phylogenetic branches that display a combination of linker features (Fig. 1A; Fig. S1). First, we identified two BRX family genes in the early diverging angiosperm lineage, *Amborella trichopoda* (*AmbBRXL1* and *AmbBRXL2*). Both encoded proteins have linkers of a size comparable with *A. thaliana* BRX family proteins (125 and 120 amino acids, respectively) and, in both, the 20-amino-acid motif is conserved. However, only AmbBRXL2 carries the R(D/E)S consensus phosphosite (Fig. S1). When expressed under control of the *AtBRX* promoter, an AmbBRXL1-CITRINE fusion protein codon-optimized for *A. thaliana* only partially complemented the root growth (Fig. S2A) or protophloem defects (Fig. S2B) of *A. thaliana brx* mutants. By contrast, a codon-optimized AmbBRXL2-CITRINE fusion protein fully complemented all *brx* mutant defects (Fig. S2C,D) and, consistently, AmbBRXL2, but not AmbBRXL1, displayed auxin-induced plasma-membrane dissociation (Fig. S2K-M). These functional assays reiterate the importance of the S228 phosphosite for AtBRX-like activity.

Next, using the same complementation approach, we monitored three BRX family proteins identified in bryophytes, the two proteins identified in the *Physcomitrium patens* genome (PpBRXL1 and PpBRXL2), and the single protein found in the *Marchantia polymorpha* genome (MpBRXL1). All three proteins lack the R(D/E)S phosphosite as well as the 20-amino-acid motif; however, whereas PpBRXL1 and PpBRXL2 linker sizes are comparable with those of *A. thaliana* BRX family proteins (127 and 122 amino acids, respectively), the MpBRXL1 linker is considerably shorter (61 amino acids) (Fig. S1). As expected, all three proteins only partially rescued the root growth vigor or protophloem defects of *brx* mutants (Fig. S2E-J), and none of them were auxin-responsive (Fig. S2N-P). As all five proteins assayed displayed protophloem-specific expression and polar localization similar to AtBRX (Fig. S2Q-U), we conclude that the linker sequence between the BRX-domains is a major determinant of specific activity, consistent with previous findings (Beuchat et al., 2010a; Koh et al., 2021), and that the entire functional spectrum represented by AtBRX is only contained in a subgroup of angiosperm BRX family proteins.

Seedling growth vigor is enhanced by heterologous SmBRX expression

Our assays of bryophyte BRX family proteins reiterate that the linker region contains the functional features that make AtBRX unique and are required for proper protophloem sieve element differentiation (Koh et al., 2021). Notably, however, neither of the three bryophyte proteins consistently conferred wild-type levels of root growth vigor observed previously in complementation experiments with SmBRX (Koh et al., 2021), which has the shortest (37 amino acids) linker identified so far and lacks any of the conserved linker sequences recognizable in most other BRX family proteins (Fig. 1A; supplementary Dataset 1). To further explore this phenomenon, we expressed the SmBRX-CITRINE fusion protein under the control of the *AtBRX* promoter in the wild-type background. Corroborating its growth-promoting effect, these transgenic lines displayed significantly increased growth vigor that manifested in ∼25% longer roots in 7-day-old seedlings (Fig. 1B). Such root growth promotion was not observed in similar experiments with AmbBRXL1, MpBRXL1 and AtBRXL1 (Fig. 1C-E), upon copy number increase of AtBRXL1 or AtBRXL2 (Fig. 1F,G), or upon ectopic overexpression of AtBRX or AtBRXL2 under control of the ubiquitous *35S* promoter (Fig. 1H,I). To exclude that the growth-promoting property of SmBRX was due to its codon optimization for *A. thaliana*, we introduced a similar construct expressing a non-codon-optimized version ($SmBRX^{nop}$) into *brx* mutants and Col-0 wild type. Similar to codon-optimized SmBRX, this protein displayed sieve element-specific expression and polar localization (Fig. S2V). Again, we observed partial complementation of protophloem defects and levels of root growth vigor in *brx* similar to those of wild type (Fig. S3A,B), and levels of root growth vigor in Col-0 that were larger than those of wild type (Fig. S3C). Conversely, a codon-optimized version of AtBRX ($AtBRX^{opt}$) behaved like the wild-type protein (Fig. S3D-F). In summary, these experiments suggest that structural features of the SmBRX protein are responsible for its growth-promoting property.

Next, we tested whether SmBRX mediates enhanced root growth across a range of conditions. We found that both wild-type and

Development (2022) 149, dev200917. doi:10.1242/dev.200917

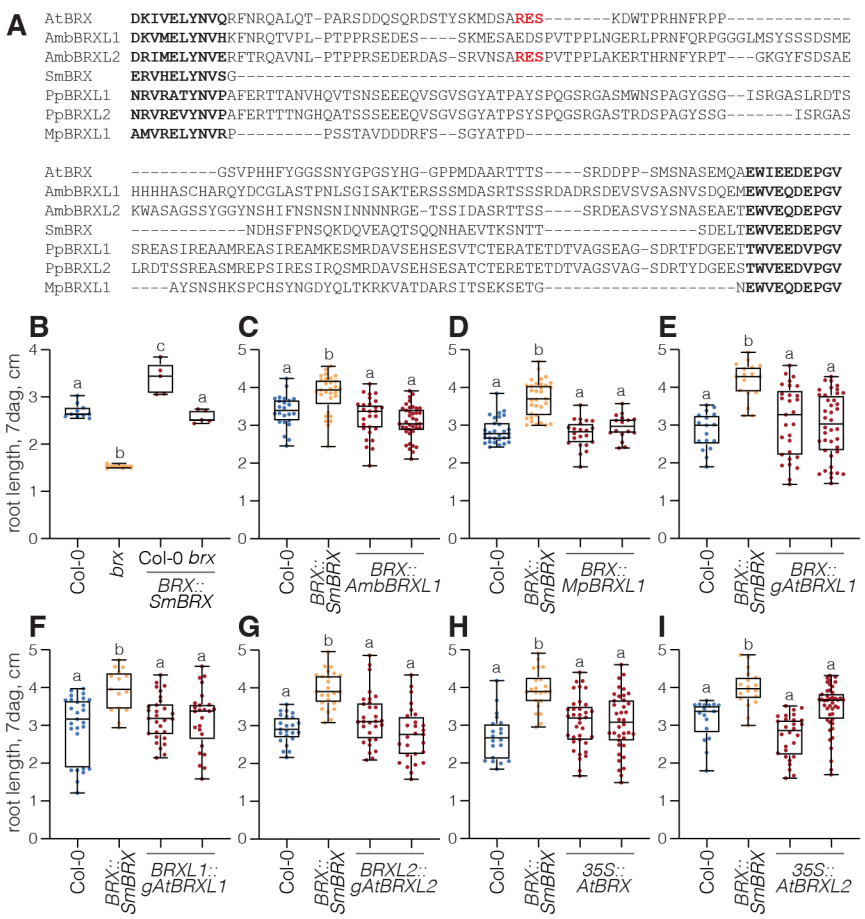

Fig. 1. Heterologous expression of the *Selaginella moellendorffii* BRX family protein enhances root growth vigor. (A) Alignment of the linker in BRX family proteins (flanked by ten amino acids of each flanking BRX-domain in bold) from *Arabidopsis thaliana* (AtBRX), *Amborella trichopoda* (AmbBRXL1 and AmbBRXL2), *Selaginella moellendorffii* (SmBRX), *Physcomitrium patens* (PpBRXL1 and PpBRXL2) and *Marchantia polymorpha* (MpBRXL1). The AGC kinase target phosphosite of AtBRX and AmbBRXL2 is highlighted in red. (B) Average root length of 7-day-old seedlings from Col-0 wild-type, *brx* mutant and transgenic lines expressing the *S. moellendorffii BRX* homolog under control of the *A. thaliana BRX* promoter (*BRX::SmBRX*). *n*=5-10 independent (transgenic) lines and experiments. (C-E) Root length of 7-day-old seedlings from Col-0, *brx* and two representative independent transgenic lines each, expressing the indicated BRX family proteins under control of the *A. thaliana BRX* promoter in Col-0. *n*=24-39 roots (C); *n*=17-33 roots (D); *n*=17-40 roots (E). (F,G) Root length of 7-day-old seedlings from Col-0, *brx* and two representative independent transgenic lines with a dosage increase in the indicated *A. thaliana BRX* family gene in Col-0. *n*=15-29 roots (F); *n*=23-30 roots (G). (H,I) Root length of 7-day-old seedlings from Col-0, *brx* and two representative independent transgenic lines each, ectopically overexpressing the indicated *A. thaliana* BRX family protein under the control of the constitutive *35S* promoter in Col-0. *n*=20-38 roots (H); *n*=17-44 roots (I). Box plots display the second and third quartiles and the median, and the whiskers indicate the maximum and minimum. All BRX family proteins were expressed as C-terminal CITRINE fusions. Statistically significant different samples (lowercase letters) were determined by ordinary one-way ANOVA with Tukey's post hoc test. Days after germination, dag.

SmBRX transgenics responded to variations in sucrose concentration in the medium; however, in all conditions, the SmBRX transgenics displayed longer roots than those of wild type (Fig. 2A-C). The difference in growth vigor was even amplified in the absence of sucrose (Fig. 2A). Likewise, SmBRX transgenics maintained their growth advantage in various adverse conditions, such as in the absence of any nutrients (Fig. 2D), sub-optimal pH (Fig. 2E) or when challenged by peptides that suppress protophloem formation (Depuydt et al., 2013) (Fig. 2F). Although Col-0 seeds are non-dormant, we stimulated germination by application of gibberellic acid to exclude that the root growth differences could result from premature germination of SmBRX trangenics (Fig. 2G). Finally, SmBRX transgenics also kept their advantage when treated with the gibberellic acid antagonist abscisic acid (Topham et al., 2017) (Fig. S4A). In summary, our experiments suggest that heterologous expression of SmBRX in *A. thaliana* results in a robust increase in seedling growth vigor.

SmBRX confers increased seed and embryo size

To determine whether the growth advantage of SmBRX transgenics in tissue culture translates into the soil environment, we first tested the capacity of their roots to vertically penetrate a ∼2 cm thick barrier of densely packed pebbles embedded in medium. In this assay, SmBRX transgenics performed as well as the wild type (Fig. 2H), suggesting that they maintained their capacity to navigate a complex environment. We then monitored adult root system growth in a greenhouse setting. In replicate experiments with a setup of 96 tubes, SmBRX transgenics maintained their growth advantage until at least 31 days after germination. However, the difference in the mean root length between wild type and SmBRX transgenics remained relatively constant in comparisons between 21-day-old (Fig. 2I) and 31-day-old (Fig. 2J) plants (between 3 and 4 cm, with the average wild-type length ∼28 and 37 cm, respectively), suggesting that SmBRX transgenics do not display a permanently higher growth rate but might carry over an early advantage. As we had excluded a causative role of premature or accelerated germination (Fig. 2G), we closely inspected the seeds. Indeed, seeds from SmBRX transgenics were visibly bigger than wild-type seeds (Fig. 2K). Size approximation through image analysis of flatbed scans of dried seeds confirmed this notion and its statistical significance for a sample of independent transgenic lines and wild-type seed batches harvested at different times (Fig. 2L,M). By contrast, seed batches of *brx* mutants were similar in size to wild type (Fig. 2L,M). Moreover, a high-resolution image analysis (Fig. S4B,C) of thousands of individual seeds confirmed these results for a comparison of wild type with independent transgenic lines that expressed either an AtBRX-CITRINE fusion protein or an SmBRX-CITRINE fusion protein under the control of the *AtBRX* promoter. The distributions of surface projection (Fig. 3A), maximum seed length (Fig. 3B) and maximum seed width (Fig. 3C) were largely similar for wild type and AtBRX transgenics, whereas the distributions of all parameters tested for SmBRX transgenics were skewed to higher values (Fig. 3A-C). Based on the average length and width, we estimated that the derived idealized ellipsoid

Development (2022) 149, dev200917. doi:10.1242/dev.200917

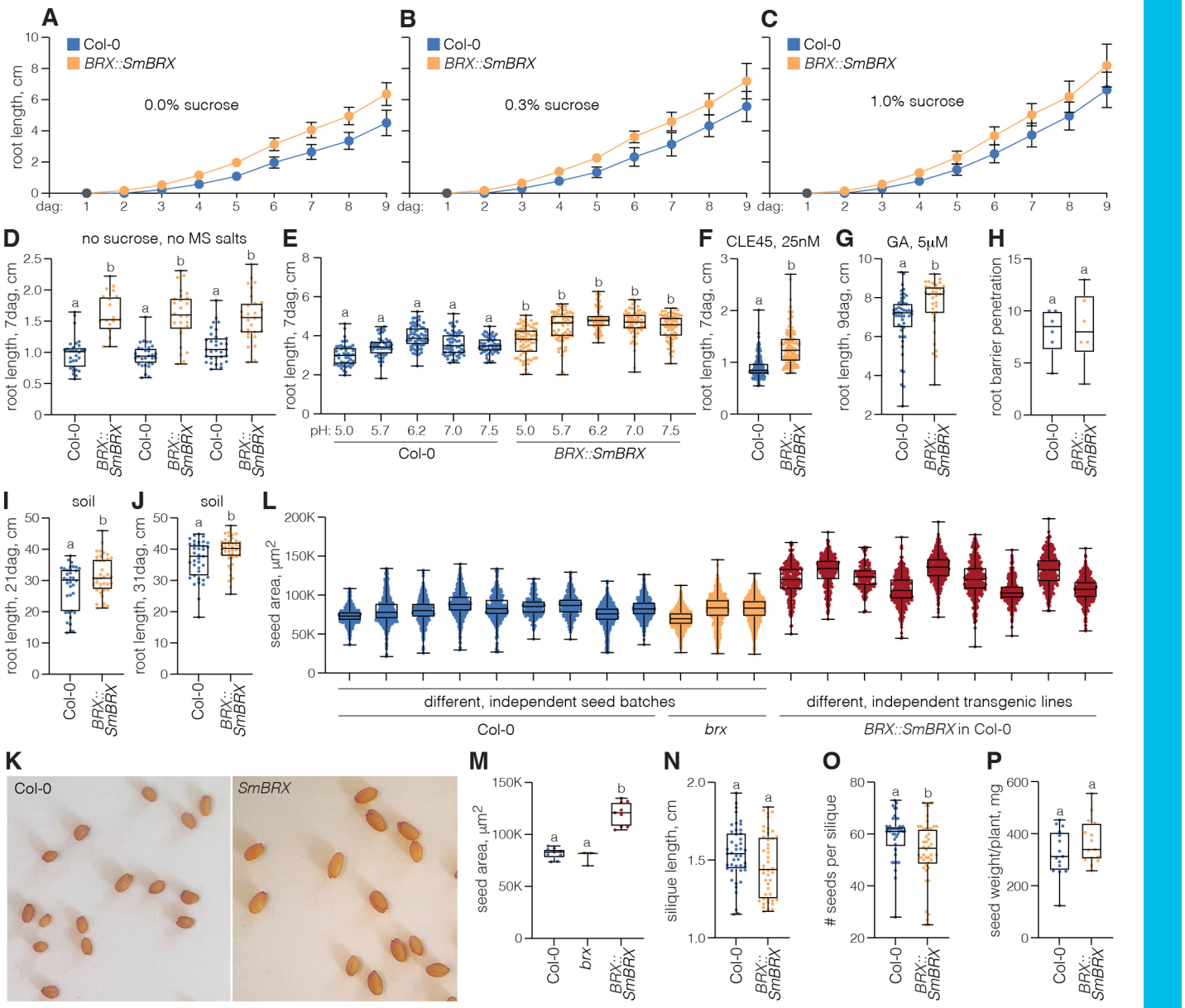

Fig. 2. Enhanced seedling vigor in lines expressing SmBRX is robust. (A-C) Root growth progression in Col-0 wild-type and transgenic lines expressing the *S. moellendorffii BRX* homolog under the control of the *A. thaliana BRX* promoter in Col-0 (*BRX::SmBRX*), on medium with different sucrose supplements. *n*=30-51 roots per time point. Error bars indicate s.d. (D) Root length of 7-day-old seedlings from Col-0 and *BRX::SmBRX* plants, grown on plain agar medium, three independent seed batches each. *n*=19-32 roots. (E-G) Root length of 7- or 9-day-old seedlings from Col-0 and *BRX::SmBRX* plants, grown on medium adjusted for different pH (E) or supplemented with CLE45 peptide (F) or gibberellic acid (GA) (G). *n*=51-74 roots (E); *n*=127-159 roots (F); *n*=35-50 roots (G). (H) Number of roots that successfully penetrated a dense ∼2 cm layer of pebbles embedded in agar medium at 10 days after germination. *n*=6 replicates, 20 plants per replicate. (I,J) Root length of 21- or 31-day-old Col-0 and *BRX::SmBRX* plants, grown in soil in individual rhizotrons. *n*=36-42 roots. Note that rhizotron length was 50 cm and *BRX::SmBRX* plants in J frequently reached the bottom of the setup box. (K) Flatbed scanner images of seeds obtained from greenhouse-grown Col-0 and *BRX::SmBRX* plants, equal scale. (L) Projected area of Col-0, *brx* and *BRX::SmBRX* seeds in flatbed scanner images, for seed batches harvested from independent lines at different times. *n*=357-628 seeds. (M) Projected area of Col-0, *brx* and *BRX::SmBRX* seeds in flatbed scanner images, shown as averages per genotype for the data shown in L. *n*=3-9. (N-P) Silique length (N), seed number per silique (O) and total dry seed weight per plant (P) for greenhouse-grown Col-0 and *BRX::SmBRX* plants. *n*=45 siliques each (N); *n*=41-44 siliques (O); *n*=15 plants each (P). Box plots display the second and third quartiles and the median, and the whiskers indicate the maximum and minimum. Statistically significant different samples (lowercase letters) were determined by ordinary one-way ANOVA with Tukey's post hoc test.

seed volume of SmBRX transgenics is increased by about 75% compared with that of wild type or AtBRX transgenics (∼0.190 µm^3 versus ∼0.107 µm^3). In summary, our data suggest that the seeds of SmBRX transgenics are substantially bigger than those of wild type. Dried *A. thaliana* seeds largely represent the mature embryo, because the endosperm is consumed as embryogenesis progresses (Doll and Ingram, 2022; Lafon-Placette and Köhler, 2014). This suggests that mature SmBRX transgenic embryos would be bigger than wild-type embryos, which turned out to be the case (Fig. 4A,B). Finally, this observation matches the reported activity of the *AtBRX* promoter during embryogenesis (Bauby et al., 2007; Scacchi et al., 2009). Investigation of SmBRX transgenics by confocal microscopy imaging matched these earlier findings and revealed expression of the SmBRX-CITRINE fusion

Development (2022) 149, dev200917. doi:10.1242/dev.200917

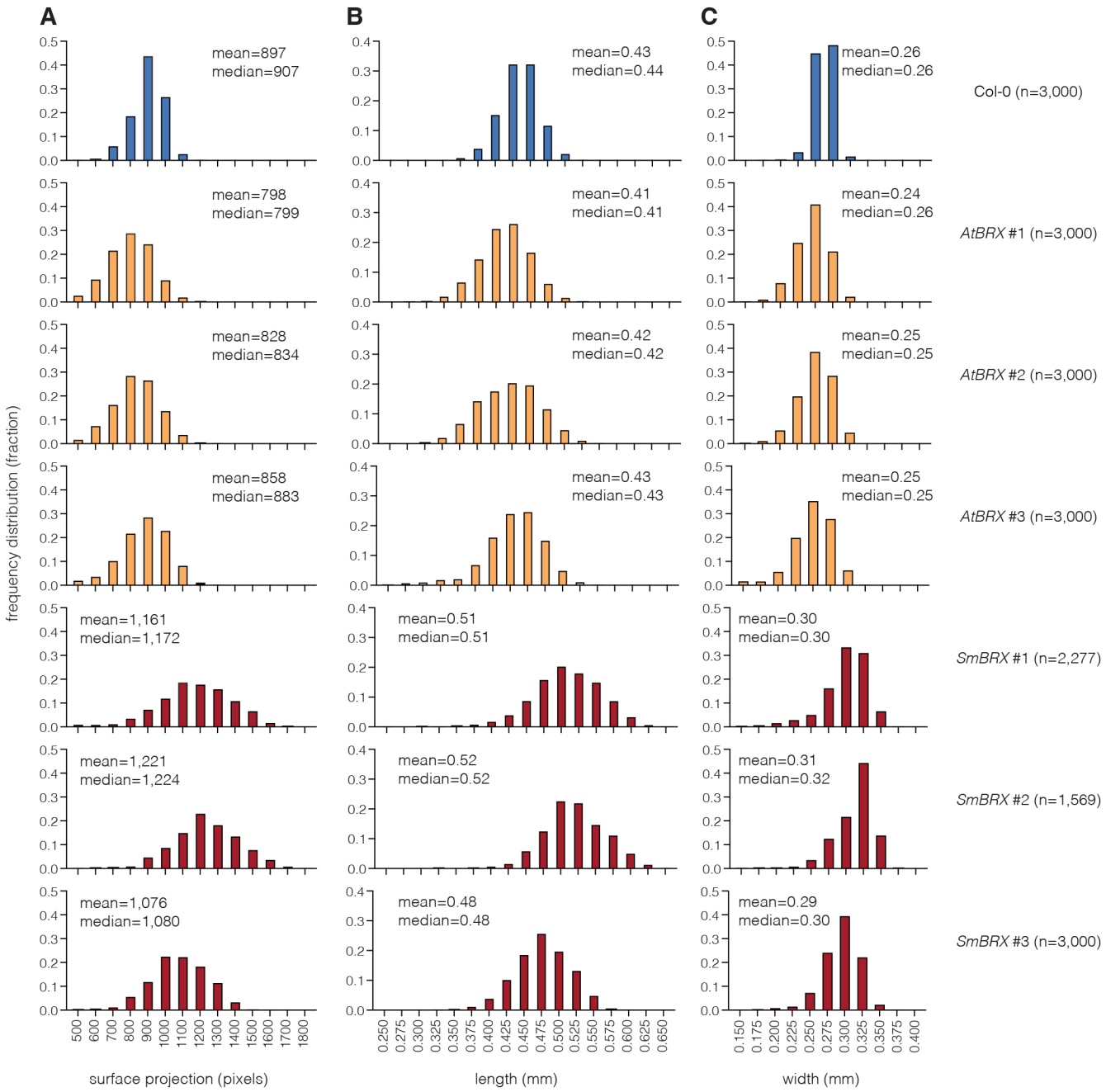

Fig. 3. Heterologous SmBRX confers increased seed size. (A-C) High-throughput, high-resolution seed size parameter measurements obtained on the Boxeed platform for Col-0 wild-type and three independent transgenic lines each expressing either AtBRX or SmBRX under control of the *A. thaliana* BRX promoter in Col-0 background. Dry seeds were harvested from mother plants grown in parallel.

protein in the shoot apical meristem of early and late heart-stage embryos (Fig. 4C,D) that ceased in the torpedo stage (Fig. 4E), whereas expression in the developing (phloem) vasculature of the hypocotyl-root axis and the cotyledons was observed from the bent cotyledon stage onwards (Fig. 4F) and persisted in maturing embryos (Fig. 4G,H). Moreover, stele width, measured at the hypocotyl-radicle junction, was significantly larger in SmBRX transgenics than in wild type (Fig. 4I). Consistently, cell counts across tissue layers showed an increase specifically in vascular cell files in SmBRX transgenics (Fig. 4J), which might thus drive the size increase.

Next, we asked whether the increased seed size in SmBRX transgenics is associated with tradeoffs in seed or in biomass productivity. In greenhouse-grown plants, we did not observe any difference in fruit size (silique length, Fig. 2N); however, we observed a statistically significant, ∼10% reduction in seed number (Fig. 2O). Nevertheless, total dry seed weight per plant was similar, if not in tendency slightly greater, in SmBRX transgenics (Fig. 2P). Collectively, our data suggest that the *SmBRX* transgene triggers a substantial increase in seed size, accompanied by a small decrease in seed number, but does not adversely affect overall plant productivity.

Development (2022) 149, dev200917. doi:10.1242/dev.200917

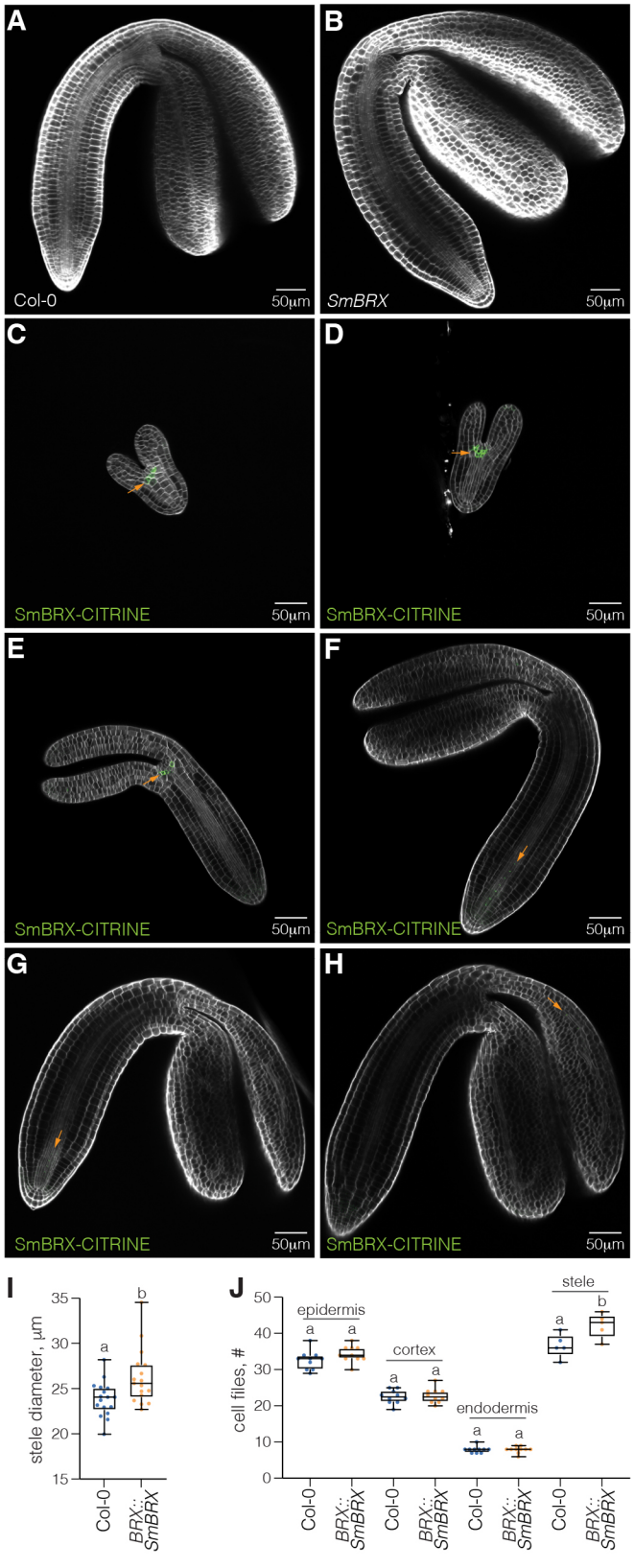

Fig. 4. SmBRX expression in embryogenesis. (A,B) Confocal microscopy images of Calcofluor White-stained mature embryos, dissected from a Col-0 (A) or SmBRX transgenic seed (B). (C-H) Confocal microscopy images of SmBRX-CITRINE fusion protein (green fluorescence) expression (orange arrows) in Calcofluor White-stained SmBRX transgenic embryos, in early (C) or late (D) heart stage, torpedo stage (E), bent cotyledon stage (F) or maturing embryos (G,H). G and H show different confocal planes of the same embryo. (I,J) Stele width (I) and cell file counts (J) at the hypocotyl-radicle junction of mature embryos. *n*=17 (I) or 10 (J) mature embryos. Box plots display the second and third quartiles and the median, and the whiskers indicate the maximum and minimum. Statistically significant different samples (lowercase letters) were determined by ordinary one-way ANOVA with Tukey's post hoc test.

An AtBRX in-frame deletion variant recapitulates SmBRX gain-of-function effects

Because SmBRX diverges from AtBRX not only in the linker between the BRX domains, but also in the non-conserved sequences that connect the conserved domains in the N-terminal regions, we sought to determine whether the reduced linker size of 37 amino acids was causative for the SmBRX-mediated growth promotion. To this end, we engineered an AtBRX variant in which residues 219 to 266 were deleted, thereby removing the 20-amino-acid motif including the RES phosphosite (Fig. S1) and reducing the linker size from 93 to 45 amino acids. This 'SmBRX-like' AtBRX (AtBRX^{Sml}) was then introduced into Col-0 wild-type plants and *brx* mutants as a CITRINE fusion protein, expressed under the control of the *AtBRX* promoter. Intriguingly, AtBRX^{Sml} transgenics displayed similar features as SmBRX transgenics. In the *brx* background, protophloem defects were only partially rescued (Fig. 5A), although root growth vigor was similar to that of wild type (Fig. 5B); in the wild-type background, AtBRX^{Sml} promoted root elongation as much as SmBRX (Fig. 5C) and, again, this could be traced back to a bigger seed size (Fig. 5D). In summary, these data suggest that removal of the regulatory phosphosite in conjunction with a size reduction in the linker between the BRX domains confers a dominant, growth-promoting effect on AtBRX.

DISCUSSION

Plants represent a variation of eukaryotic multicellularity that is distinct from animals in its unique structural, physiological and cellular characteristics. They evolved independently and it is therefore not surprising that their genomes encode proteins that are specific to the green lineage (Armisén et al., 2008; Guo, 2013; Jiao et al., 2020; One Thousand Plant Transcriptomes Initiative, 2019; Rensing, 2020). The BRX family proteins are a prime example in this context, as their highly conserved domains are not found outside plants. Besides the two conserved domains in the N-terminal half of BRX proteins, the tandem BRX domains in the C-terminal half are the most prominent and a single BRX domain can also be found in another plant-specific group of proteins that typically also contain, among others, a lipid-binding domain (Briggs et al., 2006; Furutani et al., 2020; van Leeuwen et al., 2004). The exact molecular function of the BRX-domains remains somewhat obscure, but evidence from various independent studies suggests that they primarily mediate both homologous and heterologous protein-protein interactions and membrane attachment (Briggs et al., 2006; Furutani et al., 2020; Li et al., 2019; Marhava et al., 2020; Wang et al., 2022). BRX domains might therefore primarily represent versatile scaffolds to recruit other proteins to the plasma membrane and/or regulate their trafficking, which could explain their involvement in various processes, such as subcellular polarity establishment and the maintenance or modulation of phytohormone transport (Furutani et al., 2020; Li et al., 2019; Marhava et al., 2020; Marhava et al., 2018; Moret et al., 2020; Muroyama et al., 2020).

Development (2022) 149, dev200917. doi:10.1242/dev.200917

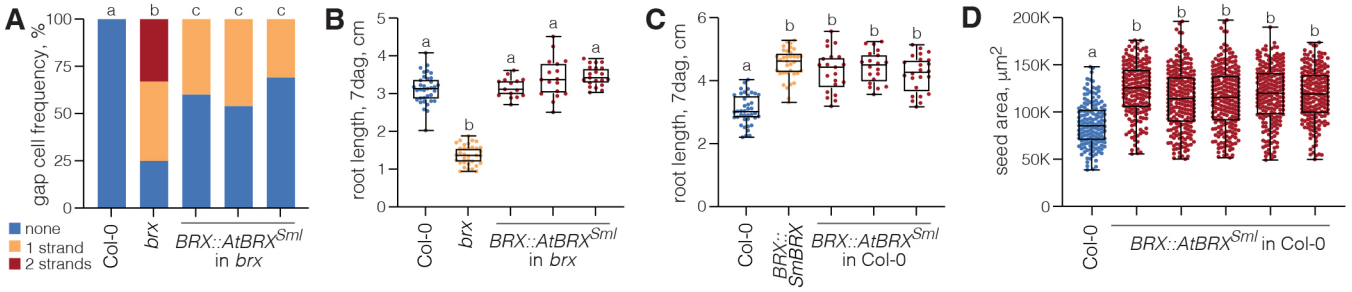

Fig. 5. An AtBRX variant recapitulates SmBRX gain-of-function effects. (A) Quantification of protophloem sieve element differentiation defects ('gap cells') in 7-day-old roots from Col-0 wild-type, *brx* mutant and three independent transgenic lines expressing an AtBRX variant with an in-frame deletion of amino acids 219-266 (AtBRX^{sml}) under the control of the *A. thaliana BRX* promoter in the *brx* background. *n*=24-36 roots. (B) Root length of 7-day-old seedlings corresponding to the genotypes assayed in A. *n*=15-35 roots. (C) Root length of 7-day-old Col-0 seedlings and transgenic seedlings expressing either SmBRX or AtBRX^{sml} under the control of the *A. thaliana BRX* promoter in Col-0. *n*=20-40 roots. (D) Projected area of seeds from Col-0 and five independent transgenic AtBRX^{sml} lines in flatbed scanner images, for seed batches harvested from mother plants grown in parallel. *n*=147-216 seeds. Box plots display the second and third quartiles and the median, and the whiskers indicate the maximum and minimum. Statistically significant different samples (lowercase letters) were determined by Fisher's exact test (A) or ordinary one-way ANOVA with Tukey's post hoc test (B-D).

The founding member of the BRX protein family in *A. thaliana* was identified via a loss-of-function allele, through a natural variation approach (Mouchel et al., 2004). Thus, despite the high conservation of AtBRX and its essential role in root protophloem development (Aliaga Fandino and Hardtke, 2022; Rodriguez-Villalon et al., 2014), the *AtBRX* gene is apparently dispensable in particular circumstances. Indeed, additional, extant loss-of-function alleles isolated from natural settings suggest that in acidic soils, where root growth is generally inhibited, such alleles might even confer a competitive advantage (Gujas et al., 2012). Conversely, *AtBRX* was also identified as a quantitative trait locus that conferred slightly yet significantly increased root growth vigor (Beuchat et al., 2010a). The underlying, causative, natural *AtBRX* allele carries a small, seven-amino-acid in-frame deletion in the linker between the BRX domains (Beuchat et al., 2010a). This deletion does not affect the phosphosite that is necessary for comprehensive AtBRX function in the protophloem (Koh et al., 2021), but supports the conclusion from our current study that the linker has a pivotal influence on the activity of BRX family proteins.

Among the BRX family proteins that we identified, SmBRX has the shortest linker sequence and lacks the crucial phosphosite required to fully replace AtBRX in root protophloem development (Koh et al., 2021). However, additional, heterologous SmBRX expression in *A. thaliana* wild type confers increased seed and embryo size, and subsequently enhanced seedling vigor. The engineered AtBRX^{sml} variant, which we synthesized using AtBRX as the backbone, has the same effects in both Col-0 wild-type and *brx* mutant backgrounds. This supports the idea that the unique amino acid sequence of SmBRX is not responsible for the observed gain-of-function effects, but rather structural features that depend on the distance between the two BRX domains. Notably, this effect was observed upon expression of SmBRX under the control of the relatively weak *AtBRX* promoter (Bauby et al., 2007; Beuchat et al., 2010b; Scacchi et al., 2009). However, whether the observed gain-of-function effects are directly related to the expression in the protophloem remains unclear, because the *AtBRX* promoter confers initially wider expression during embryogenesis (including the apical shoot meristem and the root stem cell niche) (Bauby et al., 2007; Scacchi et al., 2009) and because, importantly, the gene body also shapes the *AtBRX* expression pattern (Koh et al., 2021). Nevertheless, the observed SmBRX protein expression pattern in embryogenesis is consistent with the increased vascular proliferation, and also with the observation that *AtBRX* loss-of-function mutants display smaller cotyledons (Beuchat et al., 2010b).

Interestingly, the knock-out allele of *brx* in Col-0 background used in this study was originally identified because of its hypersensitive response to the phytohormone abscisic acid (Rodrigues et al., 2009). One of the various biological functions of abscisic acid is the promotion of seed dormancy; however, our experiments do not support premature or accelerated germination as causative for enhanced seedling root growth upon SmBRX or AtBRX^{sml} expression. Nevertheless, SmBRX/AtBRX^{sml}-conferred gain of function might reflect reduced abscisic acid sensitivity, because loss-of-function mutants in the downstream abscisic acid effector ABSCISIC ACID-INSENSITIVE 5 (ABI5) form bigger seeds (Cheng et al., 2014; Li and Li, 2016), and because gibberellic acid, an abscisic acid antagonist, promotes post-germination root meristem growth (Achard et al., 2009; Moubayidin et al., 2010). However, our observation that SmBRX transgenics respond normally to abscisic acid does not support this scenario. Nevertheless, these leads could be investigated in follow-up experiments, which might also clarify why exactly SmBRX/AtBRX^{sml} seeds are bigger, as multiple interactions between the seed coat, endosperm and embryo contribute to the final outcome of seed development (Doll and Ingram, 2022; Lafon-Placette and Köhler, 2014; Li and Li, 2016). Given the high conservation of BRX family proteins in both non-vascular and non-seed plants, such analyses might also aid in the characterization of their ancestral function. Phylogenetic analyses of linker sequence evolution could yield additional insight and clarify whether there is an evolutionary trend in linker length or sequence. Protein homology searches suggest that within the euphyllophytes, BRX family proteins are prevalent in angiosperms and might be less common in gymnosperms or ferns. This could, however, also reflect sampling bias (One Thousand Plant Transcriptomes Initiative, 2019). Combined with experimental verification, phylogenetic analyses could also clarify whether there is a threshold linker length or an absent sequence feature associated with the gain-of-function effect, which could, for example, explain why it was not observed with the relatively short linker of MpBRXL1. Finally, irrespective of the mechanism through which the SmBRX/AtBRX^{sml} gain of function operates, and which we did not identify here, our data suggest that BRX family protein variants might be applied as tools to robustly modify seedling vigor without yield penalty.

Development (2022) 149, dev200917. doi:10.1242/dev.200917

MATERIALS AND METHODS

Sequences

The protein sequences analyzed in this paper are provided in supplementary Dataset 1. The open reading frame coding sequences used for the creation of transgenes are provided in supplementary Dataset 2.

Plant material and growth conditions

The *A. thaliana* Columbia-0 (Col-0) accession was the wild-type background for all lines produced in this study. Transgenes were assayed in Col-0 or the *brx-2* mutant allele (Rodrigues et al., 2009) background. For tissue culture phenotyping assays, seeds were surface sterilized and then stratified for 2 days in the dark at 4°C. Seeds were then germinated and grown in continuous white light of ∼120 µmol·m^{-2}·s^{-1} intensity at 22°C, on vertically placed Petri dishes that contained 0.5× Murashige and Skoog (MS) medium supplemented with 1% agar and 0.3% sucrose, or variations as indicated by the labels in figure panels. Adult plants were either monitored under controlled conditions in a walk-in chamber (16 h light/8 h dark cycle with ∼130 µmol·m^{-2}·s^{-1} light intensity, 22°C, 60% humidity) or a greenhouse (16 h light/8 h dark cycle with variable light intensity between ∼120 and ∼360 µmol·m^{-2}·s^{-1}, 24°C, 50% humidity). For treatments, medium was supplemented with synthesized CLE45 peptide (Genscript) or gibberellic acid (Sigma-Aldrich).

Generation of transgenic lines

Transgenic constructs for plant transformation were created in the pH7m34GW binary vector (Addgene plasmid #133747) using the Gateway cloning technology as previously described for *AtBRX* and *SmBRX* (Koh et al., 2021). The coding sequences for the BRX family proteins and variants assayed in this study are provided in the supplementary Dataset 2. DNA fragments for transgene construction were either obtained by gene synthesis (*AtBRX*^{opt}, *AtBRX*^{Sml}, *AmbBRXL1*, *AmbBRXL2* and *MpBRXL1*) (GeneArt, using the codon optimization tool where pertinent), or by reverse transcription PCR amplification from mRNA isolated from *P. patens* or *S. moellendorffii* plants using standard procedures (*SmBRX*^{nop}, *PpBRXL1* and *PpBRXL2*). All BRX family protein variants tested were expressed as C-terminal CITRINE fusion proteins to permit verification of transgene expression. All binary constructs were verified by Sanger sequencing and introduced into the *Agrobacterium tumefaciens* strain GV3101pMP90 for plant transformation using the floral dip method.

Phenotyping

For root length or seed size measurements, plates or seeds were imaged using a high resolution (1200 dpi) flatbed scanner. Seedling root length or seed area was determined with Fiji image analysis software (version 2.0.1/1.53i), using suitable plugins. For the quantification of gap cells in protophloem sieve element cell files or visualization of fluorescent protein localization, roots were imaged by confocal microscopy as previously described (Koh et al., 2021). High-throughput and high-resolution seed size measurements were performed on the Boxeed platform run by Labdeers (https://www.labdeers.com). For trait quantification in adult *A. thaliana*, plants were grown in soil individually, in 50 cm-long open-ended polyvinyl chloride tubes of 3.5 cm diameter, which were arranged in a 96 (8×12) setup. The tubes were lined with thin plastic sheets to facilitate removal of the root system and subsequent careful soil washout. Root systems were then imaged together with a ruler under a fixed-distance camera setup and measured. Shoot productivity (seed number, silique length and seed weight) was monitored at the end of life. All phenotyping assays were performed using homozygous T3 or T4 transgenic lines with verified transgene expression. Staining and confocal microscopy were performed as previously described (Koh et al., 2021).

Embryo microscopy and cellular analysis

To visualize the SmBRX-CITRINE fusion protein during embryogenesis, embryos at different developmental stages were excised, fixed, cleared and stained as previously described (Imoto et al., 2021). For cell counts and other quantitative measures, mature embryos were dissected, fixed, stained and imaged as previously described (Bassel et al., 2014; Truernit et al., 2008). Images were acquired with a Leica Stellaris 5 confocal microscope.

Sequence analyses

BRX family protein sequences were retrieved from the 'One KP' transcriptome dataset (One Thousand Plant Transcriptomes Initiative, 2019) and aligned and analyzed using SnapGene software (version 6.0.2).

Quantification and statistical analysis

Analyses to determine statistical significance were performed in Graphpad Prism software, version 9.3.1. Specific statistical tests used are indicated in the figure legends and were always two-tailed.

Acknowledgements

The authors would like to thank Prof. T. Beeckman for *Selaginella moellendorffii* plants and A. Amiguet-Vercher for technical support.

Competing interests

The authors declare no competing or financial interests.

Author contributions

Conceptualization: S.W.H.K., C.S.H.; Methodology: S.W.H.K., H.N.D.-A.; Validation: S.W.H.K., H.N.D.-A., C.S.B., E.B.; Investigation: S.W.H.K., H.N.D.-A., E.B., C.S.B.; Resources: C.S.B.; Writing - original draft: S.W.H.K., C.S.H.; Writing - review & editing: S.W.H.K., G.I., M.E., C.S.H.; Visualization: S.W.H.K., H.N.D.-A., C.S.H.; Supervision: G.I., M.E., C.S.H.; Funding acquisition: M.E., C.S.H.

Funding

This study was funded by the Swiss National Science Foundation (Schweizerischer Nationalfonds zur Förderung der Wissenschaftlichen Forschung) grant 310030B_185379 awarded to C.S.H.

Peer review history

The peer review history is available online at https://journals.biologists.com/dev/lookup/doi/10.1242/dev.200917.reviewer-comments.pdf.

References

Achard, P., Gusti, A., Cheminant, S., Alioua, M., Dhondt, S., Coppens, F., Beemster, G. T. S. and Genschik, P. (2009). Gibberellin signaling controls cell proliferation rate in Arabidopsis. *Curr. Biol.* **19**, 1188-1193. doi:10.1016/j.cub.2009.05.059

Aliaga Fandino, A. C. and Hardtke, C. S. (2022). Auxin transport in developing protophloem: a case study in canalization. *J. Plant Physiol.* **269**, 153594. doi:10.1016/j.jplph.2021.153594

Amborella Genome Project. (2013). The Amborella genome and the evolution of flowering plants. *Science* **342**, 1241089. doi:10.1126/science.1241089

Anne, P. and Hardtke, C. S. (2018). Phloem function and development-biophysics meets genetics. *Curr. Opin. Plant Biol.* **43**, 22-28. doi:10.1016/j.pbi.2017.12.005

Armisén, D., Lecharny, A. and Aubourg, S. (2008). Unique genes in plants: specificities and conserved features throughout evolution. *BMC Evol. Biol.* **8**, 280. doi:10.1186/1471-2148-8-280

Bassel, G. W., Stamm, P., Mosca, G., Barbier de Reuille, P., Gibbs, D. J., Winter, R., Janka, A., Holdsworth, M. J. and Smith, R. S. (2014). Mechanical constraints imposed by 3D cellular geometry and arrangement modulate growth patterns in the Arabidopsis embryo. *Proc. Natl. Acad. Sci. USA* **111**, 8685-8690. doi:10.1073/pnas.1404616111

Bassukas, A. E. L., Xiao, Y. and Schwechheimer, C. (2021). Phosphorylation control of PIN auxin transporters. *Curr. Opin. Plant Biol.* **65**, 102146. doi:10.1016/j.pbi.2021.102146

Bauby, H., Divol, F., Truernit, E., Grandjean, O. and Palauqui, J.-C. (2007). Protophloem differentiation in early Arabidopsis thaliana development. *Plant Cell Physiol.* **48**, 97-109. doi:10.1093/pcp/pcl045

Beuchat, J., Li, S., Ragni, L., Shindo, C., Kohn, M. H. and Hardtke, C. S. (2010a). A hyperactive quantitative trait locus allele of Arabidopsis BRX contributes to natural variation in root growth vigor. *Proc. Natl. Acad. Sci. USA* **107**, 8475-8480. doi:10.1073/pnas.0913207107

Beuchat, J., Scacchi, E., Tarkowska, D., Ragni, L., Strnad, M. and Hardtke, C. S. (2010b). BRX promotes Arabidopsis shoot growth. *New Phytol.* **188**, 23-29. doi:10.1111/j.1469-8137.2010.03387.x

Breda, A. S., Hazak, O. and Hardtke, C. S. (2017). Phosphosite charge rather than shootward localization determines OCTOPUS activity in root protophloem. *Proc. Natl. Acad. Sci. USA* **114**, E5721-E5730. doi:10.1073/pnas.1703258114

Briggs, G. C., Mouchel, C. F. and Hardtke, C. S. (2006). Characterization of the plant-specific BREVIS RADIX gene family reveals limited genetic redundancy

despite high sequence conservation. *Plant Physiol.* **140**, 1306-1316. doi:10.1104/pp.105.075382

Bringmann, M. and Bergmann, D. C. (2017). Tissue-wide mechanical forces influence the polarity of stomatal stem cells in arabidopsis. *Curr. Biol.* **27**, 877-883. doi:10.1016/j.cub.2017.01.059

Cheng, Z. J., Zhao, X. Y., Shao, X. X., Wang, F., Zhou, C., Liu, Y. G., Zhang, Y. and Zhang, X. S. (2014). Abscisic acid regulates early seed development in Arabidopsis by ABI5-mediated transcription of SHORT HYPOCOTYL UNDER BLUE1. *Plant Cell* **26**, 1053-1068. doi:10.1105/tpc.113.121566

Depuydt, S., Rodriguez-Villalon, A., Santuari, L., Wyser-Rmili, C., Ragni, L. and Hardtke, C. S. (2013). Suppression of Arabidopsis protophloem differentiation and root meristem growth by CLE45 requires the receptor-like kinase BAM3. *Proc. Natl. Acad. Sci. USA* **110**, 7074-7079. doi:10.1073/pnas.1222314110

Doll, N. M. and Ingram, G. C. (2022). Embryo-endosperm interactions. *Annu. Rev. Plant Biol.* **73**, 293-321. doi:10.1146/annurev-arplant-102820-091838

Furutani, M., Hirano, Y., Nishimura, T., Nakamura, M., Taniguchi, M., Suzuki, K., Oshida, R., Kondo, C., Sun, S., Kato, K. et al. (2020). Polar recruitment of RLD by LAZY1-like protein during gravity signaling in root branch angle control. *Nat. Commun.* **11**, 76. doi:10.1038/s41467-019-13729-7

Gujas, B., Alonso-Blanco, C. and Hardtke, C. S. (2012). Natural arabidopsis brx loss-of-function alleles confer root adaptation to acidic soil. *Curr. Biol.* **22**, 1962-1968. doi:10.1016/j.cub.2012.08.026

Guo, Y.-L. (2013). Gene family evolution in green plants with emphasis on the origination and evolution of Arabidopsis thaliana genes. *Plant J.* **73**, 941-951. doi:10.1111/tpj.12089

Imoto, A., Yamada, M., Sakamoto, T., Okuyama, A., Ishida, T., Sawa, S. and Aida, M. (2021). A clearsee-based clearing protocol for 3D visualization of Arabidopsis thaliana embryos. *Plants (Basel)* **10**, 190. doi:10.3390/plants10020190

Jiao, C., Sorensen, I., Sun, X., Sun, H., Behar, H., Alseekh, S., Philippe, G., Palacio Lopez, K., Sun, L., Reed, R. et al. (2020). The *Penium margaritaceum* genome: hallmarks of the origins of land plants. *Cell* **181**, 1097-1111.e1012. doi:10.1016/j.cell.2020.04.019

Koh, S. W. H., Marhava, P., Rana, S., Graf, A., Moret, B., Bassukas, A. E. L., Zourelidou, M., Kolb, M., Hammes, U. Z., Schwechheimer, C. et al. (2021). Mapping and engineering of auxin-induced plasma membrane dissociation in BRX family proteins. *Plant Cell* **33**, 1945-1960. doi:10.1093/plcell/koab076

Lafon-Placette, C. and Köhler, C. (2014). Embryo and endosperm, partners in seed development. *Curr. Opin. Plant Biol.* **17**, 64-69. doi:10.1016/j.pbi.2013.11.008

Li, N. and Li, Y. (2016). Signaling pathways of seed size control in plants. *Curr. Opin. Plant Biol.* **33**, 23-32. doi:10.1016/j.pbi.2016.05.008

Li, Z., Liang, Y., Yuan, Y., Wang, L., Meng, X., Xiong, G., Zhou, J., Cai, Y., Han, N., Hua, L. et al. (2019). OsBRXL4 regulates shoot gravitropism and rice tiller angle through affecting LAZY1 nuclear localization. *Mol. Plant* **12**, 1143-1156. doi:10.1016/j.molp.2019.05.014

Marhava, P., Bassukas, A. E. L., Zourelidou, M., Kolb, M., Moret, B., Fastner, A., Schulze, W. X., Cattaneo, P., Hammes, U. Z., Schwechheimer, C. et al. (2018). A molecular rheostat adjusts auxin flux to promote root protophloem differentiation. *Nature* **558**, 297-300. doi:10.1038/s41586-018-0186-z

Marhava, P., Aliaga Fandino, A. C., Koh, S. W. H., Jelínková, A., Kolb, M., Janacek, D. P., Breda, A. S., Cattaneo, P., Hammes, U. Z., Petrášek, J. et al. (2020). Plasma membrane domain patterning and self-reinforcing polarity in Arabidopsis. *Dev. Cell* **52**, 223-235.e225. doi:10.1016/j.devcel.2019.11.015

Moret, B., Marhava, P., Aliaga Fandino, A. C., Hardtke, C. S. and Ten Tusscher, K. H. W. (2020). Local auxin competition explains fragmented differentiation patterns. *Nat. Commun.* **11**, 2965. doi:10.1038/s41467-020-16803-7

Moubayidin, L., Perilli, S., Dello Ioio, R., Di Mambro, R., Costantino, P. and Sabatini, S. (2010). The rate of cell differentiation controls the Arabidopsis root meristem growth phase. *Curr. Biol.* **20**, 1138-1143. doi:10.1016/j.cub.2010.05.035

Mouchel, C. F., Briggs, G. C. and Hardtke, C. S. (2004). Natural genetic variation in Arabidopsis identifies BREVIS RADIX, a novel regulator of cell proliferation and elongation in the root. *Genes Dev.* **18**, 700-714. doi:10.1101/gad.1187704

Muroyama, A., Gong, Y. and Bergmann, D. C. (2020). Opposing, polarity-driven nuclear migrations underpin asymmetric divisions to pattern Arabidopsis stomata. *Curr. Biol.* **30**, 4467-4475.e4464. doi:10.1016/j.cub.2020.08.100

One Thousand Plant Transcriptomes Initiative. (2019). One thousand plant transcriptomes and the phylogenomics of green plants. *Nature* **574**, 679-685. doi:10.1038/s41586-019-1693-2

Pfannebecker, K. C., Lange, M., Rupp, O. and Becker, A. (2017). Seed plant-specific gene lineages involved in carpel development. *Mol. Biol. Evol.* **34**, 925-942. doi:10.1093/molbev/msw297

Rensing, S. A. (2020). How plants conquered land. *Cell* **181**, 964-966. doi:10.1016/j.cell.2020.05.011

Rodrigues, A., Santiago, J., Rubio, S., Saez, A., Osmont, K. S., Gadea, J., Hardtke, C. S. and Rodriguez, P. L. (2009). The short-rooted phenotype of the brevis radix mutant partly reflects root abscisic acid hypersensitivity. *Plant Physiol.* **149**, 1917-1928. doi:10.1104/pp.108.133819

Rodriguez-Villalon, A., Gujas, B., Kang, Y. H., Breda, A. S., Cattaneo, P., Depuydt, S. and Hardtke, C. S. (2014). Molecular genetic framework for protophloem formation. *Proc. Natl. Acad. Sci. USA* **111**, 11551-11556. doi:10.1073/pnas.1407337111

Scacchi, E., Osmont, K. S., Beuchat, J., Salinas, P., Navarrete-Gómez, M., Trigueros, M., Ferrandiz, C. and Hardtke, C. S. (2009). Dynamic, auxin-responsive plasma membrane-to-nucleus movement of Arabidopsis BRX. *Development* **136**, 2059-2067. doi:10.1242/dev.035444

Shindo, C., Bernasconi, G. and Hardtke, C. S. (2008). Intraspecific competition reveals conditional fitness effects of single gene polymorphism at the Arabidopsis root growth regulator BRX. *New Phytol.* **180**, 71-80. doi:10.1111/j.1469-8137.2008.02553.x

Spencer, V., Nemec Venza, Z. and Harrison, C. J. (2021). What can lycophytes teach us about plant evolution and development? Modern perspectives on an ancient lineage. *Evol. Dev.* **23**, 174-196. doi:10.1111/ede.12350

Topham, A. T., Taylor, R. E., Yan, D., Nambara, E., Johnston, I. G. and Bassel, G. W. (2017). Temperature variability is integrated by a spatially embedded decision-making center to break dormancy in Arabidopsis seeds. *Proc. Natl. Acad. Sci. USA* **114**, 6629-6634. doi:10.1073/pnas.1704745114

Truernit, E., Bauby, H., Dubreucq, B., Grandjean, O., Runions, J., Barthélémy, J. and Palauqui, J.-C. (2008). High-resolution whole-mount imaging of three-dimensional tissue organization and gene expression enables the study of Phloem development and structure in Arabidopsis. *Plant Cell* **20**, 1494-1503. doi:10.1105/tpc.107.056069

van Leeuwen, W., Ökrész, L., Bögre, L. and Munnik, T. (2004). Learning the lipid language of plant signalling. *Trends Plant Sci.* **9**, 378-384. doi:10.1016/j.tplants.2004.06.008

Wang, L., Li, D., Yang, K., Guo, X., Bian, C., Nishimura, T., Le, J., Morita, M. T., Bergmann, D. C. and Dong, J. (2022). Connected function of PRAF/RLD and GNOM in membrane trafficking controls intrinsic cell polarity in plants. *Nat. Commun.* **13**, 7. doi:10.1038/s41467-021-27748-w

Zhang, Y., Liang, J., Cai, X., Chen, H., Wu, J., Lin, R., Cheng, F. and Wang, X. (2021). Divergence of three BRX homoeologs in Brassica rapa and its effect on leaf morphology. *Hortic Res.* **8**, 68. doi:10.1038/s41438-021-00504-3

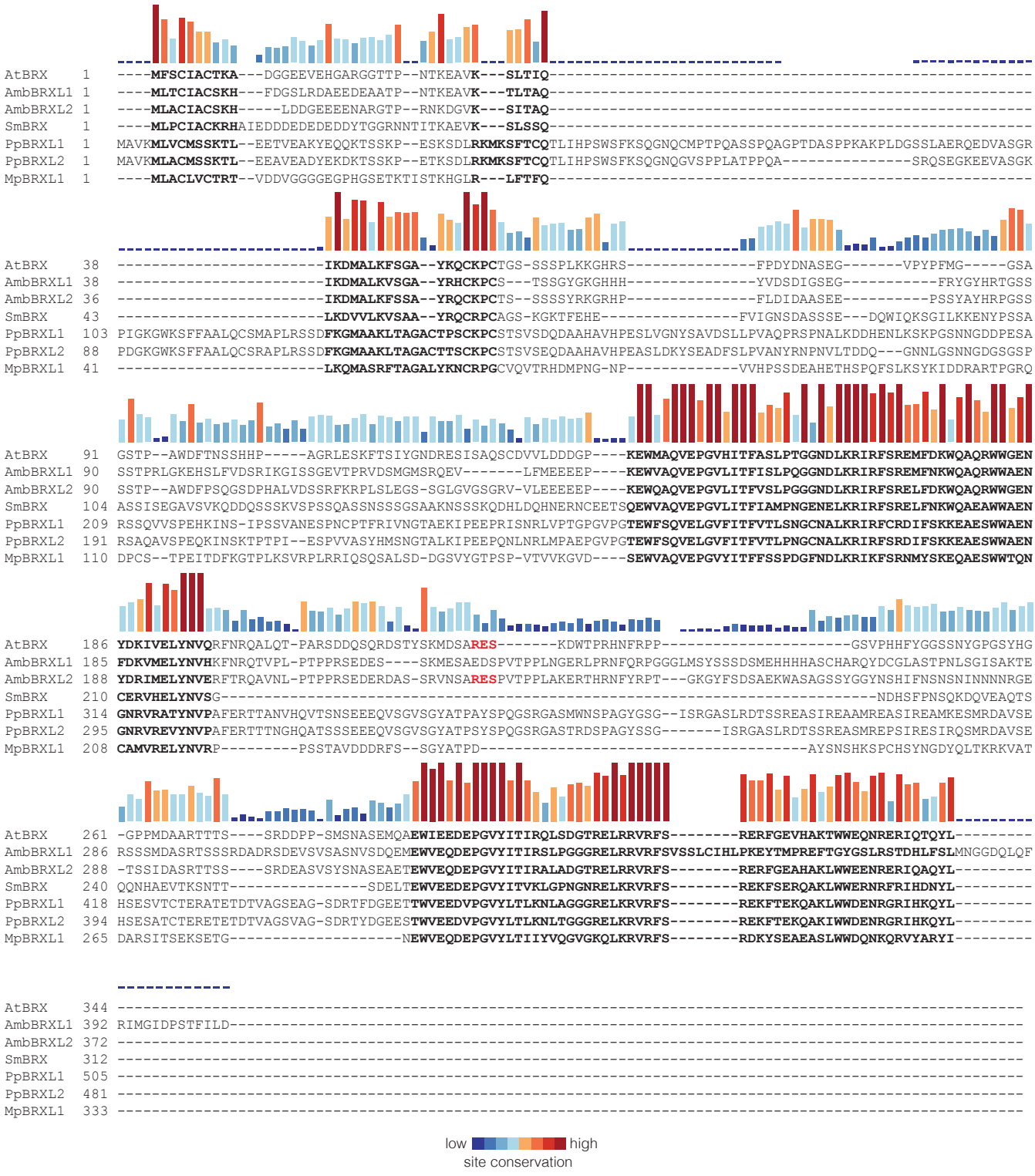

Fig. S1. Sequence alignment. Alignment of BRX family proteins from *Arabidopsis thaliana* (AtBRX), *Amborella trichopoda* (AmbBRXL1 and AmbBRXL2), *Selaginella moellendorffii* (SmBRX), *Physcomitrium patens* (PpBRXL1 and PpBRXL2), and *Marchantia polymorpha* (MpBRXL1). The AGC kinase target phosphosite of AtBRX and AmbBRXL2 in the linker between the BRX-domains is highlighted in red.

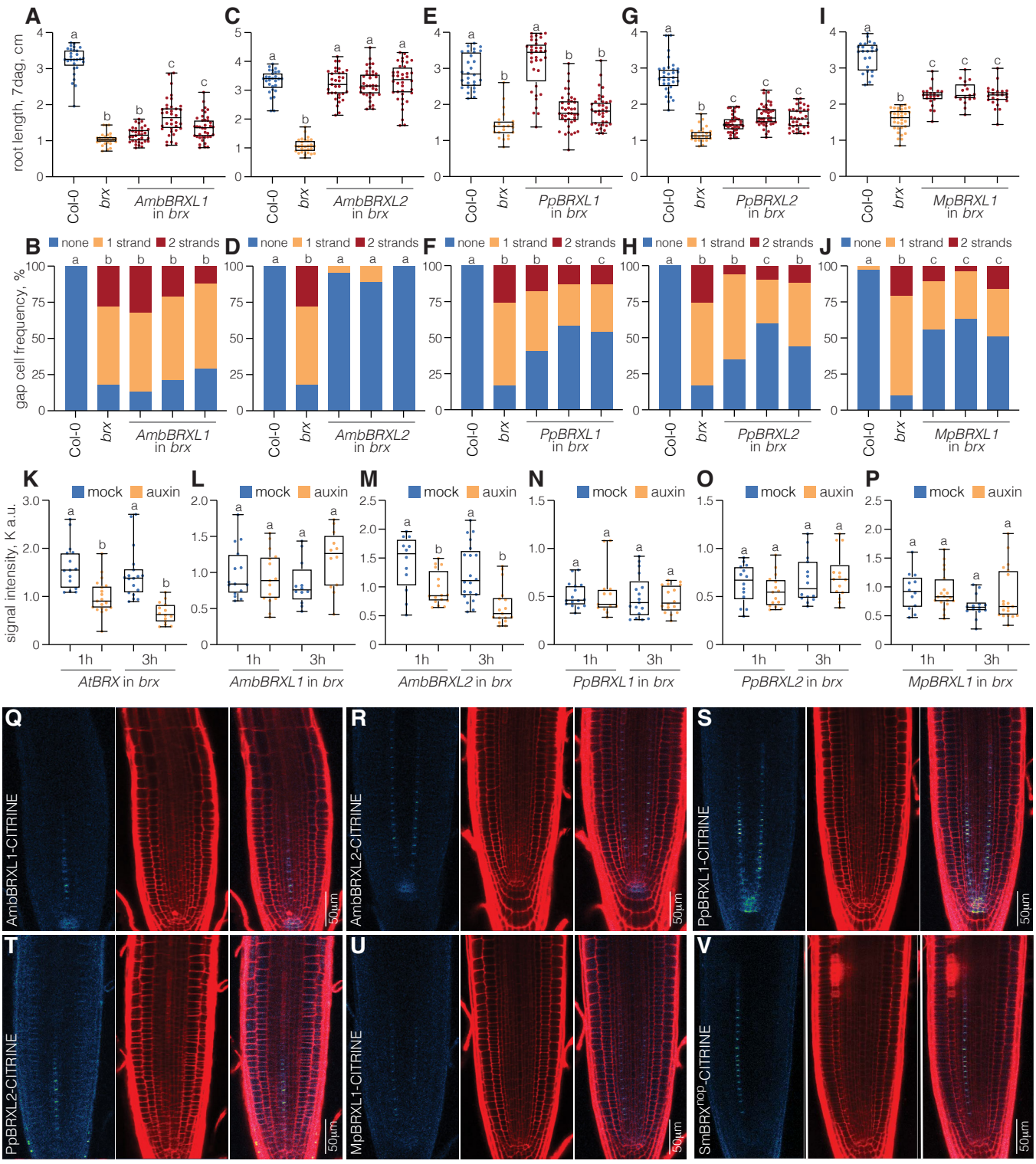

Fig. S2. Functional assays of BRX family proteins across the green lineage. (A-J) Root length of 7-day-old seedlings and corresponding quantification of protophloem sieve element differentiation defects ("gap cells") in 7-day-old roots from Col-0 wildtype, *brx* mutant, and three representative independent transgenic lines each expressing the indicated BRX family proteins under control of the *A. thaliana BRX* promoter in *brx* background. (A) n=26-38 roots; (B) n=17-31 roots; (C) n=28-38 roots; (D) n=26-41 roots; (E) n=21-40 roots; (F) n=22-31 roots; (G) n=25-40 roots; (H) n=17-25 roots; (I) n=17-33 roots; (J) n=29-45 roots. (K-P) Signal intensity quantification of indicated CITRINE fusion proteins (expressed under control of the *A. thaliana BRX* promoter) at the rootward plasma membrane of developing protophloem sieve elements, 1h or 3h after mock (DMSO) or auxin (10μM 1-naphthalene-acetic acid) treatment. (Q-V) Confocal microscopy images of indicated CITRINE fusion proteins (expressed under control of the *A. thaliana BRX* promoter), showing their protophloem-specific expression and polar localization (green fluorescence, left panels). Central panels show propidium iodide-stained cell wall outline (red fluorescence), right panels show the overlay. Box plots display 2nd and 3rd quartiles and the median, bars indicate maximum and minimum. Statistically significant different samples (lower case letters) were determined by Fisher's exact test (B, D, F, H, J) or ordinary one-way ANOVA (A, C, E, G, I, K-P).

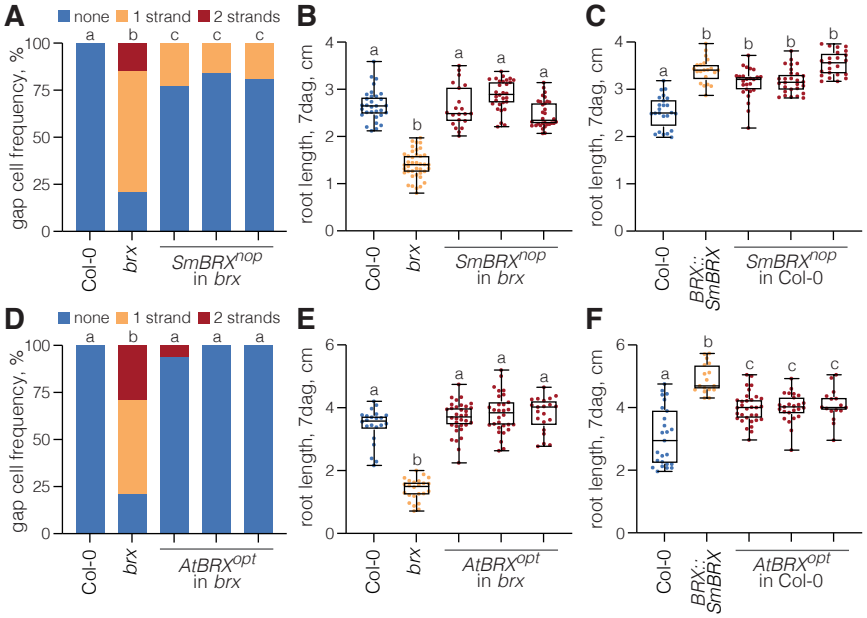

Fig. S3. Functional assays of codon-(non)-optimized SmBRX and AtBRX variants. (A) Quantification of protophloem sieve element differentiation defects ("gap cells") in 5-day-old roots from Col-0 wildtype, *brx* mutant, and three independent transgenic lines expressing a non-codon-optimized SmBRX variant ($SmBRX^{nop}$) under control of the *A. thaliana BRX* promoter in the *brx* background. n=27-48 roots. (B) Root length of 7-day-old seedlings corresponding to the genotypes assayed in (A). n=21-40 roots. (C) Root length of 7-day-old seedlings from Col-0, *brx*, and three independent transgenic lines expressing $SmBRX^{nop}$ under control of the *A. thaliana BRX* promoter in Col-0 background. n=21-28 roots. (D-F) Similar to (A-C), for an *A. thaliana* codon-optimized AtBRX variant ($AtBRX^{opt}$). (D) n=14-27 roots; (E) n=21-34 roots; (F) n=16-32 roots. Box plots display 2nd and 3rd quartiles and the median, bars indicate maximum and minimum. Statistically significant different samples (lower case letters) were determined by Fisher's exact test (A, D) or ordinary one-way ANOVA (B, C, E, F).

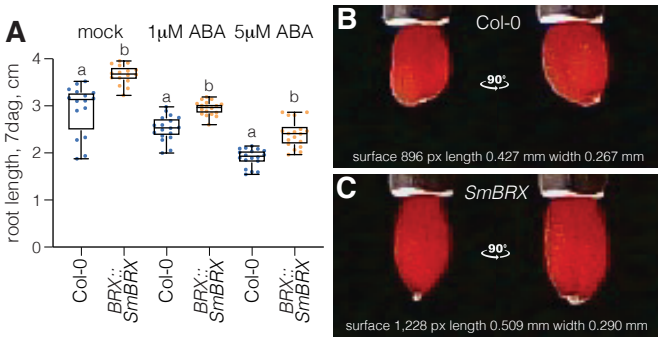

Fig. S4. Illustration of increased seed and embryo size upon heterologous SmBRX expression.

(A) Root length of 7-day-old seedlings from Col-0 and *BRX::SmBRX* plants, grown on media supplemented with increasing amounts of abscisic acid. n=16-18 roots; (B-C) Illustration of high resolution seed imaging with the *Boxeed* platform, for a Col-0 wildtype (B) and an *SmBRX* transgenic seed (C). Measured parameter values for the seeds shown are indicated.

Dataset 1. Protein sequence alignment of 302 BRX family proteins retrieved from a cross the green lineage with scaffold IDs (One Thousand Plant Transcriptomes, 2019) and species names, html file.

Click here to download Dataset 1

Dataset 2. Open reading frame coding sequences of BRX family genes and variants used for the creation of transgenes, pdf file.

AtBRX^{opt} – *Arabidopsis thaliana BRX*, codon-optimized for *A. thaliana*

ATGTTCAGCTGTATCGCTTGCACCAAGGCTGATGGTGGTGAAGAGGTTGAACATGGTGCTAGAGGTGGAACTACCCCGAACACAAAAGAGGCTGTTAAGTCCCT
CACCATCCAGATCAAGGACATGGCCCTTAAGTTCAGCGGAGCTTACAAGCAGTGCAAGCCTTGTACCGGGTCATCTTCTTCACCTCTCAAGAAGGGACACCGTAG
CTTCCCTGATTACGACAATGCTTCTGAGGGTGTGCCGTATCCTTTCATGGGAGGATCTGCTGGATCTACCCCTGCTTGGGATTTCACCAACTCTTCTCATCATCCTG
CTGGCAGGCTCGAGTCTAAGTTCACTTCTATCTACGGGAACGACCGTGAGAGCATCTCTGCTCAGTCTTGTGATGTGGTGCTCGATGACGACGGACCGAAAGAAT
GGATGGCTCAAGTTGAACCTGGTGTGCATATTACCTTCGCTTCTCTCCCTACCGGTGGAAACGATCTCAAGAGGATCAGATTCAGCCGTGAGATGTTCGACAAGT
GGCAAGCTCAAAGATGGTGGGGAGAGAACTACGACAAGATCGTCGAGCTTTACAACGTGCAGAGGTTCAACAGACAGGCTCTCCAAACTCCTGCTAGGTCTGAT
GATCAGTCTCAGAGGGACAGCACCTACAGCAAGATGGATTCTGCTCGTGAGTCTAAGGATTGGACCCCTAGACACAACTTCAGGCCTCCAGGATCTGTGCCTCAT
CATTTCTACGGCGGCTCATCTAATTACGGACCGGGATCTTATCATGGTGGACCTCCAATGGATGCTGCTAGAACTACCACCTCTTCTAGGGATGACCCTCCGTCTAT
GTCTAACGCTTCTGAGATGCAAGCTGAGTGGATCGAAGAGGATGAGCCTGGTGTGTACATCACGATCAGGCAGCTTTCTGATGGAACCAGAGAGCTTCGTCGAG
TCAGGTTCTCAAGAGAGAGGTTCGGAGAAGTTCACGCTAAGACTTGGTGGGAGCAGAACAGAGAGAGAATCCAGACTCAGTACCTC

SmBRX^{nop} – *Selaginella moellendorffii BRX*, non-optimized original sequence

ATGCTGCCTTGTATTGCTTGCAAGCGGCATGCGATTGAGGACGATGACGAAGACGAGGACGAGGACGATTACACTGGAGGCCGAAACAACACAATTACAAAGG
CCGAGGTCAAGTCCTTGTCTTCACAGCTCAAAGACGTGGTTTTGAAGGTCTCGGCCGCTTACAGGCAATGCAGGCCATGCGCTGGATCAAAGGGGAAAACTTTCG
AGCACGAATTCGTGATTGGAAACTCGGATGCTTCGTCGTCCGAGGATCAGTGGATCCAAAAGTCTGGGATTCTCAAGAAGGAGAATTATCCCAGCAGTGCTGCG
AGCTCCATCTCTGAGGGCGCAGTCTCGGTGAAACAGGACGATCAATCCAGTAGTAAAGTTTCACCGAGTAGTCAAGCGAGTAGCAACAGCAGCAGTGGATCCGC
GGCGAAGAATTCTTCTTCCAAACAAGATCATCTTGACCAACATAACGAGAGGAACTGCGAGGAGACGAGCCAGGAATGGGTGGCACAAGTCGAGCCTGGCGTTC
TTATAACTTTCATAGCAATGCCCAACGGAGAGAACGAGCTCAAGAGAATTCGATTCAGTCGCGAGCTTTTTAACAAATGGCAAGCTGAAGCATGGTGGGCCGAGA
ACTGTGAGCGTGTTCACGAGCTCTACAACGTCTCTGGAAACGATCACTCGTTTCCAAACAGCCAGAAAGATCAAGTGGAAGCACAAACGTCGCAGCAAAATCACG
CGGAAGTGACTAAATCCAACACTACGAGTGACGAACTGACCGAATGGGTCGAAGAAGACGAGCCCGGGGTTTATATCACTGTGAAGCTCGGCCCAAATGGCAAC
CGAGAACTAAAGCGTGTAAGATTCAGTCGCGAGAAGTTTAGCGAGAGGCAAGCAAAGCTATGGTGGGAGAGGAATCGCTTTAGAATACACGACAATTATTTG

AtBRX^{Sml} – "*S. moellendorffii*-like" *A. thaliana BRX*, in frame deletion of amino acids 219-266

ATGTTTTCTTGCATAGCTTGTACCAAAGCAGACGGAGGTGAAGAAGTCGAACATGGAGCGCGTGGAGGCACCACTCCCAATACTAAAGAAGCCGTCAAAAGCCT
AACCATTCAGATTAAAGATATGGCTTTGAAATTCTCTGGTGCTTATAAACAATGCAAGCCATGCACTGGTTCCTCTAGTAGTCCCTTGAAGAAAGGACATAGATCAT
TTCCGGATTATGACAATGCCTCTGAAGGTGTTCCATACCCTTTCATGGGTGGAAGTGCTGGTTCAACTCCTGCTTGGGACTTCACAAACTCCTCTCATCATCCAGCT
GGACGGTTAGAATCAAAGTTCACTTCAATATATGGAAATGATCGAGAATCTATCTCTGCACAGTCTTGTGATGTTGTACTGGATGATGATGGACCAAAAGAGTGG
ATGGCTCAAGTAGAACCTGGTGTTCATATCACATTTGCTTCTCTTCCCACTGGAGGAAATGATCTCAAACGGATCCGTTTCAGCCGAGAGATGTTTGATAAGTGGC
AAGCTCAACGGTGGTGGGGTGAGAACTATGACAAGATCGTTGAGCTTTACAATGTACAGAGATTTAACCGCCAAGCTCTCCAAACGCCTGCAAGATCCGACGATC
AGTCACAGAGAGATTCAACGGCAGCAAGAACCACAACTTCTTCCAGAGATGATCCACCTTCCATGAGCAATGCTAGTGAAATGCAAGCTGAGTGGATTGAAGAG
GACGAGCCTGGTGTTTACATTACCATCAGACAATTATCAGATGGGACTAGAGAGCTACGTCGAGTCAGATTCAGCCGGGAACGGTTTGGGGAAGTGCATGCAAA
GACATGGTGGGAGCAGAACAGAGAGAGAATACAAACACAGTACCTC

AmbBRXL1 – *Amborella trichopoda BRXL1*, codon-optimized for *A. thaliana*

ATGCTCACCTGTATCGCTTGCTCTAAGCACTTCGATGGATCTCTCAGGGATGCTGAAGAAGATGAGGCTGCTACCCCTAACACCAAAGAGGCTGTTAAGACTCTCA
CCGCTCAGATCAAGGATATGGCTCTCAAAGTGTCTGGTGCTTACAGGCATTGCAAGCCTTGCTCTACCTCTTCTGGATACGGAAAGGGACACCACCACTATGTGG
ATTCTGATATCGGATCTGAGGGATTCAGGTACGGATACCACAGAACCGGATCTTCATCTTCTACCCCTAGGCTCGGAAAAGAGCACTCACTCTTCGTTGATTCTAG
GATCAAGGGAATCTCTTCTGGTGAGGTGACCCCTAGAGTGGATTCTATGGGAATGTCTAGGCAAGAGGTTCTCTTCATGGAAGAAGAGGAACCTAAAGAGTGGG
TTGCACAGGTTGAGCCTGGTGTGCTTATTACCTTCATCTCACTTCCACAGGGTGGAAACGATCTCAAGAGGATCAGGTTCTCTAGGGAAATGTTCAACAAGTGGCA
GGCTCAGAGATGGTGGGCTGAGAACTTCGATAAGGTGATGGAACTCTACAACGTGCACAAGTTCAACAGGCAGACTGTGCCTCTTCCAACCCCTCCTAGATCTGA
GGATGAGTCATCTAAGATGGAATCTGCTGAGGATTCTCCTGTGACCCCTCCACTTAATGGTGAGAGACTCCCTAGAAACTTCCAGAGGCCTGGTGGTGGACTTAT
GTCTTACTCTTCTTCTGATTCAATGGAACATCACCACCACGCTTCATGCCACGCTAGACAATACGATTGCGGACTCGCTTCTACTCCTAACCTCTCTGGAATCTCTGC
TAAGACCGAGAGGTCTAGTTCTATGGATGCTTCTAGGACCTCTTCATCTAGGGATGCAGATAGGTCTGATGAGGTGTCAGTGTCTGCTTCTAACGTGAGTGATCA
AGAGATGGAATGGGTTGAGCAGGATGAACCTGGTGTGTATATTACTATCAGATCTCTCCCAGGTGGTGGAAGGGAACTCAGAAGAGTTAGGTTCTCTGTTTCTTC
TCTCTGCATCCACCTCCCAAAAGAGTACACCATGCCTAGGGAATTCACCGGATACGGTTCTCTCAGGTCTACCGATCATCTCTTCTCACTCATGAACGGTGGTGATC
AGCTCCAGTTCAGGATCATGGGTATCGATCCTTCAACCTTCATCCTCGAT

AmbBRXL2 – *Amborella trichopoda BRXL2*, codon-optimized for *A. thaliana*

ATGCTCGCTTGTATCGCTTGCTCTAAGCACCTCGATGATGGTGAAGAGGAAGAGAACGCTAGAGGAACCCCTAGGAACAAGGATGGTGTGAAGTCTATCACCGC
TCAGATCAAGGATATGGCTCTCAAGTTCTCTTCAGCTTACAGGCAGTGCAAGCCTTGTACCTCTTCTAGTTCTTCTTACAGAAAGGGAAGGCACCCTTTCCTTGATA
TCGATGCTGCTTCTGAGGAACCATCTTCTTACGCTTACCACAGGCCTGGATCTTCATCTTCTACTCCAGCTTGGGATTTCCCATCTCAGGGATCTGATCCTCATGCTC
TCGTGGATTCTTCTAGGTTCAAGAGGCCTTTGTCTCTCGAGGGATCTTCTGGACTTGGAGTGGGATCTGGAAGAGTTGTTCTCGAGGAAGAAGAGGAACCTAAAG
AGTGGCAAGCTCAGGTTGAGCCTGGTGTGCTTATTACCTTCGTGTCTCTTCCTGGTGGTGGAAACGATCTCAAGAGGATCAGGTTCTCTAGGGAACTCTTCGATAA
GTGGCAGGCTCAAAGATGGTGGGGAGAGAACTACGATAGGATCATGGAACTCTACAACGTGGAAAGGTTCACCAGGCAGGCTGTTAACCTTCCTACTCCTCCTA
GATCTGAGGATGAGAGGGATGCTTCTTCAAGGGTGAACTCTGCTAGGGAATCTCCTGTTACTCCTCCACTCGCTAAAGAGAGGACCCACAGAAACTTCTACAGGC
CTACTGGAAAGGGATACTTCTCTGATTCTGCTGAGAAGTGGGCTTCTGCTGGATCATCTTACGGTGGATACAACTCTCACATCTTCAACTCTAACTCTAACATTAAC
AACAACAATAGGGGAGAGACTTCTTCAATCGATGCTTCTAGGACCACCTCTAGTTCTAGGGATGAGGCTTCTGTGTCTTACTCTAACGCTTCAGAGGCTGAGACTG
AGTGGGTTGAACAAGATGAACCTGGTGTGTACATCACTATCAGGGCTCTCGCTGATGGAACCAGAGAGCTTAGAAGGGTTAGGTTCTCAAGAGAGAGGTTCGGA
GAGGCTCATGCTAAGCTTTGGTGGGAGGAAAACAGAGAGAGAATCCAGGCTCAGTACCTC

SmBRX – *S. moellendorffii BRX*, codon-optimized for *A. thaliana*

ATGCTCCCTTGTATCGCTTGCAAGAGACACGCTATCGAGGATGATGATGAGGACGAGGACGAAGATGATTACACCGGTGGACGTAACAACACCATCACTAAGGC
TGAGGTGAAGTCCCTCTCAAGCCAGCTCAAGGATGTTGTGCTCAAGGTGTCAGCTGCTTACAGACAGTGTAGACCTTGCGCTGGATCTAAGGGAAAGACTTTCGA
GCACGAGTTCGTGATCGGAAACAGCGACGCTTCTTCATCTGAGGATCAGTGGATCCAGAAGTCCGGGATCCTCAAGAAAGAGAACTACCCTAGCTCCGCCGCCTC
TTCTATTTCTGAAGGTGCTGTTTCTGTGAAGCAGGACGACCAGTCCAGCTCTAAGGTTAGCCCTTCTAGCCAGGCCTCCAGCAATTCTTCTTCTGGTTCTGCTGCCA
AGAACAGCTCCTCTAAGCAGGATCATCTCGACCAGCACAACGAGAGAAACTGCGAAGAGACTTCTCAAGAGTGGGTTGCACAAGTTGAGCCTGGTGTGCTCATC
ACCTTCATTGCTATGCCTAACGGGGAGAACGAGCTGAAGAGAATCAGGTTCTCTCGTGAGCTGTTCAACAAGTGGCAAGCTGAAGCTTGGTGGGCTGAAAACTG
TGAGAGAGTGCACGAGCTGTACAACGTGAGCGGAAACGATCACAGCTTCCCGAACTCTCAGAAGGATCAAGTTGAGGCTCAGACCAGCCAACAGAACCATGCTG
AGGTTACCAAGAGCAACACCACCTCTGATGAGCTTACTGAGTGGGTCGAAGAGGATGAACCTGGGGTTTACATCACTGTGAAGCTCGGACCTAACGGGAACAGA
GAGCTTAAGAGGGTCAGATTCAGCCGTGAGAAGTTCTCTGAGAGACAGGCTAAGCTTTGGTGGGAGAGAAACCGTTTCAGGATCCACGATAACTACCTC

PpBRXL1 – *Physcomitrium patens BRXL1*

ATGGCTGTCAAAATGTTGGTTTGCATGAGTTCGAAGACTCTGGAAGAGACCGTTGAAGCCAAATATGAGCAACAGAAGACGTCGTCGAAACCGGAGTCCAAATC
AGACTTGCGCAAAATGAAGTCGTTCACTTGCCAGACCCTGATTCATCCGTCTTGGTCTTTTAAAAGCCAAGGAAACCAATGCATGCCTACACCGCAAGCAAGTTCA
CCCCAAGCAGGTCCAACTGATGCAAGTCCGCCCAAAGCTAAGCCACTTGATGGAAGTTCTTTGGCTGAGAGACAGGAAGATGTCGCGTCCGGGAGACCTATTGG
AAAAGGCTGGAAAAGTTTTTTTGCAGCGCTACAATGCTCAATGGCACCATTACGATCCTCTGATTTTAAGGGAATGGCGGCTAAGTTGACAGCAGGAGCTTGTAC
ACCATCATGCAAGCCTTGTTCAACTTCTGTTTCTGATCAAGACGCTGCGCATGCTGTCCACCCAGAGTCTTTGGTGGGAAATTATAGTGCTGTCGATTCATTGCTAC
CAGTGGCTCAACCTCGAAGTCCTAATGCGTTGAAAGATGACCATGAAAACCTCAAGAGTAAACCCGGAAGTAATAATGGAGATGATCCAGAGTCCGCGCGGTCA
TCTCAAGTGGTCTCCCCGGAACACAAAATCAATAGCATCCCTTCCAGCGTAGCAAATGAAAGCCCGAACTGTCCAACATTCCGTATTGTGAATGGTACTGCTGAGA
AGATTCCTGAGGAGCCTCGAATTTCGAATCGTCTAGTTCCGACGGGGCCGGGTGTTCCTGGCACAGAATGGTTTTCACAAGTAGAGCTTGGAGTATTCATTACATT
CGTGACTCTGTCCAACGGTTGCAACGCACTGAAACGAATTCGATTTTGTCGAGATATTTTTAGTAAGAAAGAAGCTGAATCGTGGTGGGCGGAGAATGGAAATCG
TGTCCGCGCAACCTACAACGTGCCTGCTTTCGAAAGAACGACAGCAAATGTTCATCAAGTCACTTCAAATTCAGAAGAAGAGCAGGTATCAGGGGTTTCAGGGTA
TGCAACCCCGGCCTATAGTCCACAGGGGTCACGGGGAGCTTCAATGTGGAATTCTCCGGCTGGCTATGGTTCTGGGATATCCCGTGGAGCATCTTTGAGGGACA
CATCAAGCAGGGAAGCCTCAATCAGGGAGGCTGCAATGAGGGAAGCCTCGATTCGAGAAGCAATGAAAGAGTCTATGAGGGATGCGGTTAGCGAGCACTCTGA
ATCTGTAACTTGTACCGAAAGAGCAACCGAAACAGACACCGTTGCTGGGAGTGAGGCAGGCAGTGACAGAACTTTCGACGGAGAAGAAACTACTTGGGTTGAAG
AAGACGTTCCTGGTGTATATTTAACATTGAAGAATTTGGCCGGCGGTGGGAGAGAGTTGAAGCGTGTCAGGTTCAGCCGTGAAAAATTTACAGAGAAGCAAGCA
AAACTCTGGTGGGATGAGAACCGGGGGAGAATTCATAAACAATATCTA

PpBRXL2 – *Physcomitrium patens BRXL2*

ATGGCCGTCAAAATGCTGGCTTGCATGAGTTCGAAAACCTTGGAAGAGGCCGTCGAAGCCGACTATGAGAAGGACAAGACATCGTCCAAGCCGGAGACCAAATC
TGACTTGCGAAAAATGAAGTCATTTACTTGTCAGACCCTGATCCATCCGTCTTGGTCTTTTAAAAGCCAAGGAAATCAAGGTGTGTCCCCACCTCTAGCAACTCCAC
CTCAAGCAAGTCGTCAGTCAGAGGGAAAGGAGGAGGTCGCGTCCGGGAAACCTGATGGAAAAGGTTGGAAAAGTTTCTTTGCAGCGCTGCAATGCTCGAGGGC
ACCGCTGCGATCTTCAGACTTCAAGGGAATGGCGGCTAAGTTGACAGCAGGAGCTTGTACAACTTCTTGCAAGCCTTGTTCAACTTCTGTTTCAGAGCAAGACGCT
GCGCATGCTGTCCATCCAGAGGCTTCATTGGACAAATACAGTGAGGCTGATTTTTCGCTACCAGTGGCCAATTATCGAAATCCTAATGTGTTGACAGATGATCAAG
GAAATAACCTCGGAAGTAATAATGGAGACGGCTCAGGTTCTCCGCGTTCTGCTCAAGCGGTCTCCCCGGAGCAGAAAATCAATAGTAAAACTCCTACCCCAATTG
AAAGCCCAGTTGTTGCGAGCTATCACATGAGCAATGGAACTGCTTTGAAGATTCCTGAAGAACCTCAAAATTTGAATCGTCTTATGCCGGCTGAACCAGGTGTTCC
TGGCACTGAATGGTTTTCACAAGTAGAGCTTGGAGTATTCATAACGTTTGTGACTCTACCTAACGGTTGCAATGCTCTAAAACGAATTAGATTCAGCCGAGACATT
TTCAGCAAAAAAGAAGCTGAATCGTGGTGGGCGGAGAATGGAAATCGTGTCCGTGAAGTCTATAACGTACCAGCTTTCGAAAGGACAACGACAAATGGTCACCA
GGCTACTTCAAGTTCAGAAGAAGAGCAGGTTTCAGGGGTATCAGGGTATGCTACCCCCTCCTATAGTCCGCAGGGGTCACGAGGAGCTTCAACAAGGGATTCAC
CGGCTGGCTACAGTTCTGGGATATCGCGTGGAGCATCTTTGAGGGATACATCGAGCAGAGAGGCCTCAATGAGAGAACCGTCGATCAGAGAATCCATCAGACAG
TCGATGAGGGATGCGGTCAGCGAACATTCCGAATCCGCAACGTGTACTGAGAGAGAGACTGAAACAGATACAGTTGCTGGAAGCGTGGCAGGTAGCGACAGAA
CTTATGACGGCGAAGAATCCACTTGGGTTGAGGAAGACGTTCCTGGTGTATATTTAACATTGAAGAATTTGACTGGAGGTGGTAGAGAGTTGAAGCGTGTCAGG
TTCAGTCGTGAAAAGTTCACCGAGAAACAGGCCAAAATATGGTGGGACGAGAACCGCGGGCGAATTCACAAACAGTATCTA

MpBRXL1 – *Marchantia polymorpha BRXL1*, codon-optimized for *A. thaliana*

ATGCTTGCTTGCCTCGTGTGCACTAGAACCGTGGATGATGTTGGAGGTGGTGGTGAAGGACCTCATGGATCTGAGACTAAGACCATCTCTACCAAGCACGGGCTC
AGACTCTTCACTTTCCAGCTTAAGCAGATGGCCTCTAGGTTTACTGCTGGGGCTCTTTACAAGAACTGCAGACCTGGATGCGTTCAGGTGACCAGACATGATATGC
CTAACGGAAACCCTGTGGTGCACCCTTCATCTGATGAGGCTCATGAGACACACAGCCCTCAGTTCTCACTCAAGAGCTACAAGATCGATGACAGGGCTAGAACTC
CTGGAAGGCAGGATCCTTGTTCTACTCCTGAGATCACCGACTTCAAGGGAACCCCTCTCAAGTCTGTTAGACCTCTCAGAAGGATCCAGAGCCAGTCTGCTCTTTC
TGATGACGGATCTGTGTACGGAACTCCTTCTCCTGTTACCGTTGTGAAGGGTGTTGACTCTGAGTGGGTTGCACAAGTTGAGCCTGGTGTGTATATTACCTTCTTC
AGCAGCCCGGACGGATTCAACGATCTCAAGAGGATCAAGTTCAGCCGTAACATGTACAGCAAAGAGCAGGCTGAGTCTTGGTGGACTCAGAACTGTGCTATGGT
GCGTGAGCTTTACAACGTGAGGCCTCCTTCTTCTACCGCTGTGGATGACGATAGGTTCAGCTCTGGATACGCTACCCCTGACGCTTACTCTAACTCTCACAAGTCTC
CGTGCCACTCTTACAACGGTGATTACCAGCTCACCAAGCGTAAGGTGGCAACCGATGCTAGATCTATCACCAGCGAGAAGTCTGAGACTGGAAATGAGTGGGTC
GAGCAGGATGAACCTGGTGTTTACCTCACCATCATCTACGTGCAAGGTGTGGGAAAGCAGCTCAAGAGAGTGAGGTTCTCTAGGGACAAGTACTCTGAGGCTGA
GGCTTCTTTGTGGTGGGATCAGAACAAGCAGAGGGTGTACGCTCGTTACATC